

## Simple approach to soft-pion emission in $\bar{p}p$ interactions near threshold\*

Leo Michelotti

Department of Physics, University of California, Irvine, California 92717  
(Received 9 February 1976; revised manuscript received 28 February 1977)

Viewed in the pion rest frame, the Feynman amplitude for emission of a soft pion is simply proportional to the amplitude of the core, each possible source nucleon contributing a term proportional to its chirality. Together with threshold approximations, this observation enables us to write, in a very simple way, a general expression relating the cross section  $\sigma(\bar{p}p \rightarrow f + \pi^0)$  to  $\sigma(\bar{p}p \rightarrow f)$ , and the cross section  $\sigma(\bar{p}p \rightarrow f + \pi^+)$  to  $\sigma(\bar{p}n \rightarrow f)$ , near threshold. A comparison is made to data on the reactions  $\bar{p}p \rightarrow \bar{p}p\pi^0$ ,  $\bar{p}n\pi^+$ ,  $\bar{\Lambda}\Lambda\pi^0$ ,  $\bar{\Sigma}^-\Sigma^+\pi^0$ ,  $\bar{\Lambda}\bar{p}K^+\pi^0$ , and  $\bar{\Sigma}^+\bar{p}K^0\pi^0$ , with varying degrees of success.

### I. INTRODUCTION

Current algebra and the partial conservation of axial-vector current (PCAC) hypothesis have been used extensively over the past fifteen years to study pion emission (or absorption) within the framework of the "soft-pion" theory. In all this time, only a few papers have been devoted to soft-pion emission in  $pp$  and  $\bar{p}p$  interactions: Uritam and Nuthakki<sup>1</sup> studied the annihilation reaction  $\bar{p}p \rightarrow \bar{K}K\pi\pi$ , treating both pions as soft; Intemann and Greenhut<sup>2</sup> calculated a cross section for the process  $\bar{p}p \rightarrow \bar{K}K\pi$ ; more closely related to the present work, Beder,<sup>3</sup> Schillaci, Silbar, and Young,<sup>4</sup> and Baier and Kühnelt<sup>5</sup> all examined soft-pion production in  $pp \rightarrow NN\pi$  near threshold. In this paper, we will address single soft-pion emission in  $\bar{p}p$  interactions near threshold, with special attention to  $\bar{p}p \rightarrow \bar{B}B\pi$ .

It is important to keep these calculations as simple as possible. The *extremely* limited amount of data available and the kinematic ambiguities inherent in the theory cannot justify many complications, but a simple calculation, which can be compared to data at least in a crude way, may have some value. In addition, it is easy for involved algebraic manipulations to obscure some of the relevant threshold physics.

One simplification occurs by realizing that because a soft pion has no momentum, its effect can only be to change the spins and isospins of the other particles in the reaction, i.e., the "core" particles.<sup>6</sup> Equation (3) in Sec. II represents this mixing explicitly. In particular, when viewed in the pion rest frame, the helicity of all core nucleons is conserved. Though presumably well known, this is not often exploited in actual practice. In this helicity representation, the soft-pion amplitude for  $\pi^0$  emission is simply *proportional to the core amplitude*, each source nucleon contributing a term proportional to its chirality (velocity  $\times$  helicity). Charged-pion emission still has the added complication of mixing different isospin states, but this is a minor inconvenience in  $pp$  and  $\bar{p}p$  inter-

actions.

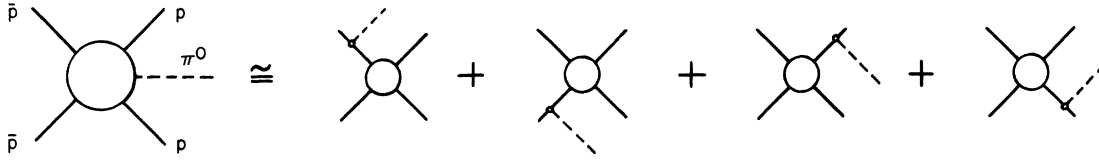
Another important simplification follows the introduction of "threshold approximations." In the pion rest frame, the velocity—and hence, the chirality—of any final-state nucleon must vanish at threshold, while the velocities of the initial-state particles have the same magnitude. For  $\pi^0$  emission, this produces cancellations in certain spin configurations; for  $\pi^\pm$  emission, it results in correlations between spin and isospin states. This correlation nullifies interference between the  $I=0$  and  $I=1$  cores in  $pp$  and  $\bar{p}p$  interactions and produces simple relationships between pion-emission cross sections and core cross sections.

But, more importantly, no particle in the final state contributes to the amplitude at threshold; that is, a threshold soft-pion amplitude contains no information about the final state. Together with our simple representation, this allows us to write an expression [Eq. (21)] applicable to a variety of processes.

We begin in Sec. II by deriving our "simplified" approach from the more familiar insertion rules of Adler.<sup>7</sup> In Sec. III this formalism is applied to  $\bar{p}p \rightarrow \bar{N}N\pi$  near threshold. Section IV contains the generalization to other final states. Finally, in Sec. V we compare the threshold predictions to data on reactions of the types  $\bar{p}p \rightarrow \bar{B}B\pi$  and  $\bar{p}p \rightarrow \bar{B}\bar{p}K\pi$ .

### II. SOFT-PION INSERTION IN THE PION REST FRAME

The first step in constructing a soft-pion amplitude is to identify the "core," which is obtained from the pion emission (or absorption) process of interest by removing the pion. A single diagram for soft-pion emission is reconstructed from the core by "inserting" the appropriate axial-vector vertex into an external particle line. The full soft-pion amplitude is then the sum over all such "insertion diagrams." As examples, and for future reference, the insertion diagrams for  $\bar{p}p \rightarrow \bar{p}p\pi^0$  and  $\bar{p}p \rightarrow \bar{p}n\pi^+$  are illustrated in Figs. 1 and 2. The core

FIG. 1. Soft-pion diagrams which contribute to  $\bar{p}p \rightarrow \bar{p}p \pi^0$ .

of the first process is the elastic-scattering reaction  $\bar{p}p \rightarrow \bar{p}p$ ; the second process also possesses the cores  $\bar{p}p \rightarrow \bar{n}n$  and  $\bar{p}n \rightarrow \bar{p}n$ .

We will restrict our attention to pion *emission*. (Diagrams for soft-pion absorption would be obtained by reversing the sign of the pion momentum and taking the Hermitian conjugate of the isospin matrices.) Further, we assume for now that the pion is inserted only into nucleons (or antinucleons), so that the isospin vertex is  $\frac{1}{2}\tau^\alpha$ . Using the usual terminology, a diagram is designated "pre-emission" or "postemission" according to whether the vertex is inserted into a particle line in the initial state or in the final state of the core.

An axial-vector insertion into a nucleon (or antinucleon) line is accomplished by making one of the following substitutions for the appropriate wave function in the core amplitude.

Preemission diagrams:

$$\bar{v}X^\dagger \rightarrow \frac{iG_A}{f_\pi} \frac{1}{2k \cdot q} [\bar{v} \not{\epsilon} \gamma^5 (\not{k} - M)] \left( X^\dagger \frac{\tau^\alpha}{2} \right), \quad (1a)$$

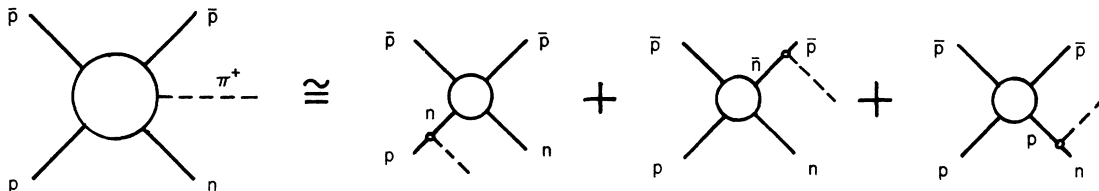
$$Xu \rightarrow -\frac{iG_A}{f_\pi} \frac{1}{2k \cdot q} \left( \frac{\tau^\alpha}{2} X \right) [(\not{k} + M) \not{\epsilon} \gamma^5 u], \quad (1b)$$

Postemission diagrams:

$$Xv \rightarrow -\frac{iG_A}{f_\pi} \frac{1}{2k \cdot q} \left( \frac{\tau^\alpha}{2} X \right) [(\not{k} - M) \not{\epsilon} \gamma^5 v], \quad (1c)$$

$$\bar{u}X^\dagger \rightarrow -\frac{iG_A}{f_\pi} \frac{1}{2k \cdot q} [\bar{u} \not{\epsilon} \gamma^5 (\not{k} + M)] \left( X^\dagger \frac{\tau^\alpha}{2} \right), \quad (1d)$$

where  $u, \bar{u}$  ( $v, \bar{v}$ ) are the Dirac spinors for the  $N(\bar{N})$ ;  $k, M$  are the four-momentum and mass of the core nucleon;  $X$  is the isospinor of the core nucleon [ $\begin{pmatrix} 1 \\ 0 \end{pmatrix}$  for  $p$  or  $\bar{p}$ ,  $\begin{pmatrix} 0 \\ 1 \end{pmatrix}$  for  $n$  or  $\bar{n}$ ];  $\alpha, q$  are the isospin index (1, 2, or 3) and momentum of the pion;  $\tau^\alpha$  are the usual Pauli matrices;  $G_A$  is the axial-vector renormalization constant ( $=C_A/C_V \cong 1.23$ );

FIG. 2. Soft-pion diagrams which contribute to  $\bar{p}p \rightarrow \bar{p}n \pi^+$ . Note that there is only one preemission diagram, in contrast to  $\bar{p}p \rightarrow \bar{p}p \pi^0$ .

and  $f_\pi$  is the pion decay constant ( $\approx 93.7$  MeV). These substitutions are considered valid only "near"  $q=0$ , or more accurately, for  $q^2 \ll k \cdot q$ . The pole at  $q=0$  comes from the new propagator created by inserting the vertex.

Although it is not usually done, it is possible to take this procedure one step further and to write the soft-pion amplitude directly as a superposition of core amplitudes. To do this, substitute into Eqs. (1) from the relations

$$\not{k} + M = \sum_{\text{spins}} u(k, s) \bar{u}(k, s), \quad (2)$$

$$\not{k} - M = \sum_{\text{spins}} v(k, s) \bar{v}(k, s).$$

These are valid when  $k^2 = M^2$ , with the normalization  $\bar{u}u = -\bar{v}v = 2M$ . The on-mass-shell condition is satisfied in the soft-pion limit.

Now, let  $\mathfrak{M}(f + \pi^\alpha | i)$  represent the soft-pion amplitude, and let  $M(f | i)$  represent a core amplitude. Note that these are the *full* Feynman amplitudes, complete with all external wave functions, and not just the form factors. We also introduce the  $2 \times 2$  spin and isospin mixing matrices

$$U_{ss'} = \frac{1}{2k \cdot q} \bar{u}(k, s) \not{\epsilon} \gamma^5 u(k, s'),$$

$$V_{ss'} = \frac{1}{2k \cdot q} \bar{v}(k, s) \not{\epsilon} \gamma^5 v(k, s'),$$

$$\left( \frac{\tau^\alpha}{2} \right)_{jj'} = X_j^\dagger \frac{\tau^\alpha}{2} X_{j'}.$$

Using these, Eqs. (2), and isospin completeness,

$$\sum_{j=n}^p X_j X_j^\dagger = 1,$$

we can write the insertion rules (1) in the forms given by the following table:

Preemission	Postemission
$N: -\frac{iG_A}{f_\pi} \sum_{j',s'} M(f i') U_{s's} \left(\frac{\tau^\alpha}{2}\right)_{j'j}$	$\frac{iG_A}{f_\pi} \sum_{j',s'} \left(\frac{\tau^\alpha}{2}\right)_{jj'} U_{ss'} M(f' i),$
$\bar{N}: \frac{iG_A}{f_\pi} \sum_{j',s'} M(f i') V_{ss'} \left(\frac{\tau^\alpha}{2}\right)_{jj'}$	$-\frac{iG_A}{f_\pi} \sum_{j',s'} \left(\frac{\tau^\alpha}{2}\right)_{j'j} V_{s's} M(f' i).$

(3)

Each entry in this table represents the contribution of one insertion diagram to the soft-pion-amplitude  $\mathfrak{M}(f+\pi^\alpha|i)$ . The subscripts  $s$  and  $j$  refer to the spin and isospin of the pion source nucleon in the final amplitude;  $s'$ ,  $j'$ ,  $i'$ , and  $f'$  symbolize the spin and isospin assignments, which must be summed, of the same nucleon in the core amplitudes.

These expressions have a natural interpretation: because a soft pion does not carry momentum, its influence can only be to mix the spins and isospins of the other particles in the reaction. The above table just represents this mixing explicitly.

The Pauli representation of  $U$  is given by

$$\begin{aligned} U_{ss'} &= \frac{1}{k \cdot q} \left( \frac{M e^0 + k}{M + k \cdot e^0} \otimes \vec{\sigma}_{ss'} \right) \cdot (q \otimes \vec{k} - k \otimes \vec{q}) \\ &= \frac{1 + M q^0 / k \cdot q}{1 + M / k^0} \vec{\sigma}_{ss'} \cdot (\vec{k} / k^0) - \frac{M q^0}{k \cdot q} \vec{\sigma}_{ss'} \cdot (\vec{q} / q^0). \end{aligned}$$

Here,  $\vec{\sigma}_{ss'} = \chi_s^\dagger \vec{\sigma} \chi_{s'}$ , and  $e^0 = (1, 0, 0, 0)$  is the unit vector in the time direction. This takes on a particularly simple form in either the pion's rest frame ( $\pi$ RF) or the nucleon's rest frame (NRF):

$$\begin{aligned} U_{ss'} &=_{\text{NRF}} -\vec{\sigma}_{ss'} \cdot (\vec{q} / q^0) \\ &= -\vec{\sigma}_{ss'} \cdot \vec{\mathcal{V}}_\pi, \\ U_{ss'} &=_{\pi\text{RF}} \vec{\sigma}_{ss'} \cdot (\vec{k} / k^0) \\ &= \vec{\sigma}_{ss'} \cdot \vec{\mathcal{V}}_N. \end{aligned} \quad (4)$$

It is more convenient to work in the  $\pi$ RF, since the NRF depends on the particular insertion diagram considered. *If the nucleon is polarized to have definite helicity  $h = \pm \frac{1}{2}$  in the  $\pi$ RF, then  $U$  is diagonal.*

$$U_{hh'} = 2\mathcal{V}_N h \delta_{hh'}; \quad \mathcal{V}_N = |\vec{\mathcal{V}}_N|, \quad h = \pm \frac{1}{2}. \quad (5)$$

Alternatively, one can interpret Eqs. (4) as follows<sup>8</sup>; because

$$\vec{\sigma} \cdot \vec{\mathcal{V}} = i\mathcal{V} \exp\left(-i\pi \frac{\vec{\sigma}}{2} \cdot \hat{\mathcal{V}}\right),$$

and similarly for  $\tau^\alpha$ , the effect of soft-pion emission on the nucleon is to rotate its spin through  $\pi$  radians—in the NRF (or the  $\pi$ RF)—about the direction  $-\vec{\mathcal{V}}_\pi$  (or  $\vec{\mathcal{V}}_N$ ), and simultaneously to rotate its isospin about the direction  $\alpha$ .

The matrix  $V$  can be obtained from  $U$  by switching the rows and columns among themselves. That

is, in an obvious notation,

$$\begin{aligned} V_{ss'} &= \bar{u}(k, s) \not{q} \gamma^5 v(k, s') \\ &= -\bar{u}(k, -s) \gamma^5 \not{q} \gamma^5 u(k, -s') \\ &= \bar{u}(k, -s) \not{q} \gamma^5 u(k, -s') \\ &= U_{-s, -s'}. \end{aligned}$$

Note that the identification  $v(k, s) = \gamma^5 u(k, -s)$  results in a phase convention not uniformly employed. Provided one remains consistent, however, there should be no error. In the helicity representation, the matrix  $V$  is then given by

$$V_{hh'} =_{\pi\text{RF}} -2\mathcal{V}_N h \delta_{hh'}. \quad (6)$$

Introducing these diagonal matrices into (3) reduces the spin sum to a single term. The isospin sum could likewise be eliminated, but it is more convenient (here) to write amplitudes explicitly for charged-pion emission. It is clear from Eqs. (3), (5), and (6) that, in the pion's rest frame, the amplitude for emission of a soft pion of definite charge can be written in the form

$$\mathfrak{M}(f+\pi|i) = \frac{iG_A}{f_\pi} \sum_{\text{insertion diagrams}} \mu Z M, \quad (7)$$

where  $M$  is the core amplitude *with nucleon charges appropriate for the diagram*, and  $Z \equiv \mathcal{V}_h$  is the chirality of the source nucleon. The value of  $\mu$  depends on the pion's charge and on the type of insertion, according to the following table:

	Preemission	Postemission
$\pi^0$ emission		
Insertion into $p$ or $\bar{p}$	-1	+1
Insertion into $n$ or $\bar{n}$	+1	-1
$\pi^-$ emission	$-\sqrt{2}$	$+\sqrt{2}$
$\pi^+$ emission	$+\sqrt{2}$	$-\sqrt{2}$

Note that Eq. (7) is still fully relativistic; no low-energy approximations were used in its derivation, apart from the soft-pion approximation itself. These will be introduced in the next section when we examine the reactions  $\bar{N}N \rightarrow \bar{N}N\pi$  near threshold.

There are a few brief remarks worth making. Although a soft pion has no energy or momentum, *it does have velocity*. Thus the soft-pion limit is

not well defined unless this velocity—or equivalently, the rest frame of the pion—is specified.

By writing the soft-pion amplitude as in Eq. (3) or (7), we are free to use any convenient phenomenological model for the core amplitudes. There is no need to write everything in terms of invariant multilinear combinations of Dirac spinors.

This “velocity×helicity” formalism is not new. It first appeared several years before the work of Adler<sup>7</sup> began to dominate soft-pion physics, when Nambu<sup>9</sup> developed this approach as a consequence of broken chiral symmetry. However, it has not been used extensively in actual calculations; that is, the spinor formulation of Eqs. (1) is generally preferred. Nonetheless, this alternative approach can be convenient, especially for doing certain “threshold” calculations, to which we now turn.

### III. SOFT-PION CALCULATIONS FOR $\bar{N}N \rightarrow \bar{N}N\pi$ NEAR THRESHOLD

Of the fourteen charge-conserving amplitudes  $\mathfrak{M}(\bar{N}_3 N_4 \pi | \bar{N}_1 N_2)$ , no more than three can be linearly independent. One possible set consists of the amplitudes for the three neutral-pion emission processes  $\bar{p}p \rightarrow \bar{p}p\pi^0$ ,  $\bar{p}n \rightarrow \bar{p}n\pi^0$ , and  $\bar{p}p \rightarrow \bar{n}n\pi^0$ . Amplitudes for the two inequivalent charged-pion reactions  $\bar{p}p \rightarrow \bar{p}n\pi^+$  and  $\bar{p}n \rightarrow \bar{p}p\pi^-$  can then be evaluated as the sums

$$\sqrt{2}\mathfrak{M}(\bar{p}n\pi^+ | \bar{p}p) = \mathfrak{M}(\bar{p}n\pi^0 | \bar{p}n) + \mathfrak{M}(\bar{n}n\pi^0 | \bar{p}p) - \mathfrak{M}(\bar{p}p\pi^0 | \bar{p}p), \quad (8)$$

$$\sqrt{2}\mathfrak{M}(\bar{p}p\pi^- | \bar{p}n) = \mathfrak{M}(\bar{p}p\pi^0 | \bar{p}p) + \mathfrak{M}(\bar{n}n\pi^0 | \bar{p}p) - \mathfrak{M}(\bar{p}n\pi^0 | \bar{p}n). \quad (9)$$

The other nine amplitudes are related to these five by either  $G$  or  $C$  invariance. (See Appendix A.)

It would suffice, then, to consider only the three processes  $\bar{p}p \rightarrow \bar{p}p\pi^0$ ,  $\bar{p}n \rightarrow \bar{p}n\pi^0$ , and  $\bar{p}p \rightarrow \bar{n}n\pi^0$ . Their soft-pion amplitudes are easily written from Eq. (7):

$$\mathfrak{M}(\bar{p}p\pi^0 | \bar{p}p) = \frac{iG_A}{f_\pi} (Z_3 + Z_4 - Z_1 - Z_2) M(\bar{p}p | \bar{p}p), \quad (10a)$$

$$\mathfrak{M}(\bar{n}n\pi^0 | \bar{p}p) = -\frac{iG_A}{f_\pi} (Z_3 + Z_4 + Z_1 + Z_2) M(\bar{n}n | \bar{p}p), \quad (10b)$$

$$\mathfrak{M}(\bar{p}n\pi^0 | \bar{p}n) = \frac{iG_A}{f_\pi} (Z_3 - Z_4 - Z_1 + Z_2) M(\bar{p}n | \bar{p}n). \quad (10c)$$

The index on  $Z$  labels the “source” nucleon for a particular insertion diagram. The indexing scheme is

$$\bar{N}_1 N_2 \rightarrow \bar{N}_3 N_4 \pi,$$

so that  $Z_1$  is the chirality of the initial antinucleon,  $Z_2$  is the chirality of the initial nucleon, and so forth.

The soft-pion amplitudes for charged-pion emission can now be calculated from Eqs. (8), (9), and (10). It is convenient to do this in terms of the isospin amplitudes  $M_0$  and  $M_1$ , where, as usual,

$$M(\bar{p}p | \bar{p}p) = \frac{1}{2}(M_0 + M_1),$$

$$M(\bar{n}n | \bar{p}p) = \frac{1}{2}(M_0 - M_1),$$

$$M(\bar{p}n | \bar{p}n) = M_1.$$

Then,

$$\sqrt{2}\mathfrak{M}(\bar{p}n\pi^+ | \bar{p}p) = \frac{iG_A}{f_\pi} [(Z_3 - Z_4 + 2Z_2)M_1 - (Z_3 + Z_4)M_0], \quad (11a)$$

$$\sqrt{2}\mathfrak{M}(\bar{p}p\pi^- | \bar{p}n) = \frac{iG_A}{f_\pi} [(2Z_4 + Z_1 - Z_2)M_1 - (Z_1 + Z_2)M_0]. \quad (11b)$$

It is easy to verify that Eqs. (11a) and (11b) can also be derived directly from Eq. (7), using the values of  $\mu$  appropriate to charged-pion emission.

Our purpose now is to explore the consequences of Eqs. (10) and (11) at energies near the pion production threshold. Accordingly, we introduce two approximations which are motivated by the idea that, at threshold, all final-state particles are at rest in the center-of-momentum frame. The first of these arises from identifying the pion’s rest frame with the c.m. frame:

$$|Z_1| = |Z_2| = p_{c.m.}/\sqrt{s}. \quad (12)$$

Here,  $p_{c.m.}$  is the initial nucleon c.m. momentum, and  $\sqrt{s}$  is the total c.m. energy. The second approximation is to set the relative velocity between the pion and either final-state nucleon at zero, which gives us

$$Z_3 = Z_4 = 0. \quad (13)$$

This corresponds to the vanishing of postemission diagrams at threshold.

Note that Eqs. (12) and (13) imply that the core amplitude refers to an inelastic, unphysical process. This in itself is not bad, but it does leave one with the problem of extrapolating off the energy shell from real-world data. We will not address this problem in detail here; its impact is somewhat lessened by phase-space averaging which comes later. (using the dispersion-theoretic approach of Fubini and Furlan,<sup>10</sup> Young,<sup>11</sup> and Banerjee *et al.*<sup>12</sup> have partially analyzed the effect of extrapolating the pion mass up to its physical value on soft-pion predictions for the reactions  $NN$

$\rightarrow NN\pi$ . Young especially pushed the analysis to the point of making some numerical estimates, but his results cannot be immediately generalized to the  $\bar{p}p$  system. At any rate, the problem of inelastic cores remains.)

Substituting the threshold approximations (12) and (13) into Eqs. (10) and (11) leads to a number of interesting predictions on the effects of polarization. Note that the two amplitudes  $\mathfrak{M}(\bar{p}p\pi^0|\bar{p}p)$  and  $\mathfrak{M}(\bar{n}n\pi^0|\bar{p}p)$  vanish at threshold when the two initial particles have opposite helicities. In contrast,  $\mathfrak{M}(\bar{p}n\pi^0|\bar{p}n)$  vanishes at threshold when the initial particles have the same helicity. Only the core  $M_1$  contributes (at threshold) to  $\mathfrak{M}(\bar{p}n\pi^+|\bar{p}p)$ , regardless of helicities; and  $\mathfrak{M}(\bar{p}p\pi^-|\bar{p}n)$  exhibits an interesting spin-isospin correlation:  $M_0$  contributes when the initial particles have the same helicity, while  $M_1$  contributes when they have opposite helicities. Since these two possibilities are mutually exclusive, *there is no interference between the  $M_1$  and  $M_0$  terms at threshold*. Unfortunately, it would be difficult to verify any of these predictions experimentally.

We will use Eq. (10a) to write the total, unpolarized cross section for  $\bar{p}p \rightarrow \bar{p}p\pi^0$ . With the normalization convention  $\bar{u}u = -\bar{v}v = 2M$ , the total cross section is

$$\begin{aligned} \sigma(\bar{p}p \rightarrow \bar{p}p\pi^0) &= \frac{(2\pi)^4}{(2\pi)^9} \frac{1}{4p_{\text{c.m.}}\sqrt{s}} \\ &\times \int d^5R_3 \frac{1}{4} \sum_{\text{spins}} |\mathfrak{M}(\bar{p}p\pi^0|\bar{p}p)|^2 \\ &= \left(\frac{1}{2\pi}\right)^5 \frac{R(\bar{p}p\pi^0)}{4p_{\text{c.m.}}\sqrt{s}} \\ &\times \frac{1}{4} \sum_{\text{spins}} \langle |\mathfrak{M}(\bar{p}p\pi^0|\bar{p}p)|^2 \rangle_3, \end{aligned} \quad (14)$$

where  $d^5R_3$  is differential three-body phase space

$$d^5R_3 = \prod_1^3 \frac{d\vec{p}}{2E} \delta^4(P_f - P_i),$$

$R(\bar{p}p\pi^0)$  is the total phase-space volume, and  $\langle \dots \rangle_3$  represents an average over three-body phase space.

When Eq. (10a), modified by the threshold approximations, is substituted into Eq. (14) and the sum over spins is done, two of the spin-triplet amplitudes—those with opposite helicities—will not contribute. Let  $\uparrow$  (or  $\downarrow$ ) represent a particle with positive (or negative) *helicity* in the center-of-mass frame. The sum over spins in Eq. (14) becomes

$$\sum_{\text{spins}} |\mathfrak{M}(\bar{p}p\pi^0|\bar{p}p)|^2 \cong \left(\frac{G_A}{f_\pi}\right)^2 \frac{4p_{\text{c.m.}}^2}{s} \sum_{\text{final spins}} [ |M(\bar{p}p|\bar{p}\uparrow p\uparrow)|^2 + |M(\bar{p}p|\bar{p}\downarrow p\downarrow)|^2 ].$$

Spin singlet and triplet amplitudes can now be introduced:

$$[M^s, M^t] = [M(\bar{p}p|\bar{p}\uparrow p\uparrow), M(\bar{p}p|\bar{p}\downarrow p\downarrow)] \begin{bmatrix} \sqrt{\frac{1}{2}} & \sqrt{\frac{1}{2}} \\ -\sqrt{\frac{1}{2}} & \sqrt{\frac{1}{2}} \end{bmatrix}.$$

Note that the labels  $s$  and  $t$  refer to particular superpositions of *initial*-state helicities, the final-state spins being unspecified. Because invariance under charge conjugation and rotation forbid singlet-triplet transitions in the core, the final spin state of  $M^s$  must be a singlet, while in  $M^t$  the final-state particles can be in any one of three possible triplet states. Two of these triplet amplitudes vanish at threshold, because the total angular momentum about the beam direction must be conserved. Therefore, right at threshold, the sum over spins reduces to only two terms. Nonetheless, for reasons which will be more apparent later, we will use the more general expression

$$\sum_{\text{spins}} |\mathfrak{M}(\bar{p}p\pi^0|\bar{p}p)|^2 \cong \left(\frac{G_A}{f_\pi}\right)^2 \frac{4p_{\text{c.m.}}^2}{s} \sum_{\text{final spins}} (|M^s|^2 + |M^t|^2). \quad (15)$$

Note again that singlet and triplet terms appear with equal weight, because interference between the two initial-particle chiralities has nullified two of the three possible triplet amplitudes.

The cross section for this process is now given by

$$\sigma(\bar{p}p \rightarrow \bar{p}p\pi^0) = \left(\frac{1}{2\pi}\right)^5 \frac{R(\bar{p}p\pi^0)}{4p_{\text{c.m.}}\sqrt{s}} \left(\frac{G_A}{f_\pi}\right)^2 \frac{4p_{\text{c.m.}}^2}{s} \frac{1}{4} \sum_{\text{final spins}} \langle |M^s(\bar{p}p|\bar{p}p)|^2 + |M^t(\bar{p}p|\bar{p}p)|^2 \rangle_3. \quad (16)$$

Our objective is to compare this to the elastic cross section

$$\sigma(\bar{p}p \rightarrow \bar{p}p) = \left(\frac{1}{2\pi}\right)^2 \frac{1}{4p_{\text{c.m.}}\sqrt{s}} R(\bar{p}p) \frac{1}{4} \sum_{\text{final spins}} \langle |M^s(\bar{p}p|\bar{p}p)|^2 + 3|M^t(\bar{p}p|\bar{p}p)|^2 \rangle_2 \cong \frac{1}{4}(\sigma^s + 3\sigma^t). \quad (17)$$

(Note the assumption that the three initial triplet states couple equally into the final states, at least in an average sense.) A major difficulty arises in doing this. Equation (16) contains off-shell amplitudes averaged over three-body phase space, while Eq. (17) contains on-shell amplitudes averaged over two-body phase space. It is not immediately clear how to relate these two. The usual approach<sup>3,4</sup> is to average the two-body cross section over the range in kinetic energy allowed to the  $\bar{p}p$  subsystem in the three-body final state. The weight function is chosen to incorporate the effects of going from two-body to three-body phase space and of bringing the amplitude off shell. Effectively, one approximates

$$\langle |M_{\text{off}}|^2 \rangle_3 \approx \frac{8}{\pi \epsilon^2} \int_0^\epsilon d\eta [\eta(\epsilon - \eta)]^{1/2} \varphi(\eta) \langle |M_{\text{on}}|^2 \rangle_2,$$

where the integration variable  $\eta$  is the kinetic energy of the  $\bar{p}p$  system,  $\epsilon = \sqrt{s} - (2M_N + m_\pi)$  is the maximum available kinetic energy, the weight factor  $(8/\pi \epsilon^2)[\eta(\epsilon - \eta)]^{1/2}$  comes from three-body non-relativistic phase space, and  $\varphi(\eta)$  is some function which changes an on-shell amplitude into an off-shell one.

With this approach, the relationship between Eqs. (16) and (17) is finally given by

$$\sigma(\bar{p}p \rightarrow \bar{p}p\pi^0) \approx \left(\frac{1}{2\pi}\right)^3 \left(\frac{G_A}{f_\pi}\right)^2 \left[ \frac{R(\bar{p}p\pi^0)}{R(\bar{p}p)} \frac{4p_{\text{c.m.}}^2}{s} \right] \times \frac{1}{4} [\bar{\sigma}^s(\bar{p}p \rightarrow \bar{p}p) + \bar{\sigma}^t(\bar{p}p \rightarrow \bar{p}p)], \quad (18)$$

where  $\bar{\sigma} = (8/\pi \epsilon^2) \int_0^\epsilon d\eta [\eta(\epsilon - \eta)]^{1/2} \varphi(\eta) \sigma(\eta)$  is the appropriately averaged core cross section. Because  $\varphi(\eta)$  is not known unambiguously, we will not pause to dwell on the details of this averaging procedure; in practice it will be done in only a crude sense.

Because Eq. (18) was derived within the framework of threshold approximations, it seems reasonable to expand the kinematic factors in square brackets to lowest order in  $\epsilon$ . The details are written down in the next section; here, we will simply lift the answer from Eq. (23). To lowest order in  $\epsilon$  and to lowest order in  $m_\pi/M_N$ ,

$$\frac{R(\bar{p}p\pi^0)}{R(\bar{p}p)} \frac{4p_{\text{c.m.}}^2}{s} \approx \frac{\sqrt{2}\pi^2}{4} \frac{m_\pi}{M_N} \epsilon^2.$$

Then, to first order, the cross section for  $\pi^0$  emission is given by

$$\sigma(\bar{p}p \rightarrow \bar{p}p\pi^0) \approx \frac{1}{32\sqrt{2}\pi} \left(\frac{G_A}{f_\pi}\right)^2 \left(\frac{m_\pi}{M_N}\right) \times \frac{1}{2} [\bar{\sigma}^s(\bar{p}p \rightarrow \bar{p}p) + \bar{\sigma}^t(\bar{p}p \rightarrow \bar{p}p)] \epsilon^2. \quad (19)$$

This is essentially the form that was reported in Burns *et al.*,<sup>13</sup> except that  $g/M_N$  was substituted for  $G_A/f_\pi$ , in accordance with the Goldberger-

Treiman relation.

Now consider the corresponding calculation for  $\pi^+$  emission, beginning from Eq. (11a). The only significant difference that arises is that, after threshold approximations are invoked, only one term survives. That is, setting  $Z_3 = Z_4 = 0$ , we have

$$\mathfrak{M}(\bar{p}n\pi^+ | \bar{p}p) \approx \sqrt{2} Z_2 M(\bar{p}n | \bar{p}n),$$

where the identification  $M_1 = M(\bar{p}n | \bar{p}n)$  has been made. Thus, unlike  $\pi^0$  emission, there is no selective cancellation of spin states, and the sum over spins becomes

$$\sum_{\text{spins}} |\mathfrak{M}(\bar{p}n\pi^+ | \bar{p}p)|^2 \approx \frac{1}{2} \left(\frac{G_A}{f_\pi}\right)^2 \frac{4p_{\text{c.m.}}^2}{s} [ |M^s(\bar{p}n | \bar{p}n)|^2 + 3 |M^t(\bar{p}n | \bar{p}n)|^2 ].$$

Comparing this to Eq. (15) shows that the  $\pi^+$  emission cross section can be obtained from Eq. (19) by replacing  $\frac{1}{2}(\sigma^s + \sigma^t)$  with  $\frac{1}{4}(\sigma^s + 3\sigma^t)$ . Thus,

$$\sigma(\bar{p}p \rightarrow \bar{p}n\pi^+) \approx \frac{1}{32\sqrt{2}\pi} \left(\frac{G_A}{f_\pi}\right)^2 \left(\frac{m_\pi}{M}\right) \times \frac{1}{4} [\bar{\sigma}^s(\bar{p}n \rightarrow \bar{p}n) + 3\bar{\sigma}^t(\bar{p}n \rightarrow \bar{p}n)] \epsilon^2. \quad (20)$$

Taken together, Eqs. (19) and (20) predict that the ratio of neutral to positively charged pion production is approximately unity:

$$R \equiv \frac{\sigma(\bar{p}p \rightarrow \bar{p}p\pi^0)}{\sigma(\bar{p}p \rightarrow \bar{p}n\pi^+)} = \frac{\frac{1}{2} [\bar{\sigma}^s(\bar{p}p \rightarrow \bar{p}p) + \bar{\sigma}^t(\bar{p}p \rightarrow \bar{p}p)]}{\frac{1}{4} [\bar{\sigma}^s(\bar{p}n \rightarrow \bar{p}n) + 3\bar{\sigma}^t(\bar{p}n \rightarrow \bar{p}n)]} \approx 1.$$

However, it is important to note that this prediction is not unique to soft-pion theory. For example, it would be obtained from any model in which the  $\pi^+$  is emitted preferentially from only a single isospin- $\frac{1}{2}$  line, but the  $\pi^0$  is emitted equally from two such lines, with negligible interference between the two diagrams. The experimental ratio  $\sigma(\bar{p}p \rightarrow \bar{p}p)/\sigma(\bar{p}p \rightarrow \bar{p}n) \approx 6$  (weakly) suggests that this might happen in a  $N^*(1, 1)$  production model. That is, we might conjecture that  $\sigma(\bar{p}p \rightarrow \bar{p}N^*)/\sigma(\bar{p}p \rightarrow \bar{N}^*n) \approx 6$ , so that a  $\pi^+$  would preferentially be emitted from a  $N^*$  line.

Although they seem similar, such an effect would be legitimately different from what occurred in the threshold soft-pion calculation.<sup>14</sup> There, for the two spin states in which there was constructive interference in the  $\pi^0$  amplitude, the amplitude was  $\sqrt{2}$  times that for  $\pi^+$  emission, but this was offset

by destructive interference in the other two spin states (i.e., four initial spin states contributed to  $\pi^+$  emission, but only two contributed to  $\pi^0$  emission). The net effect was thus to equalize the two cross sections.

A crude statistical calculation predicts  $R = \frac{4}{5}$  (see Appendix A), which would also be difficult to distinguish from  $R = 1$ . In contrast, the  $\Delta(3, 3)$  production model predicts  $R = 2$ .

Experimentally,  $R \cong 1$  for  $P_{\text{beam}} \leq 1.05$  GeV/c or  $P_{\text{beam}} \geq 1.50$  GeV/c. Between these two energies,  $R$  rises quickly to 2 (or larger), and then falls slowly until it is again approximately 1.

#### IV. A QUICK GENERALIZATION AND THE LOW-ENERGY EXPANSION

Since postemission diagrams do not contribute to the soft-pion amplitude at threshold, Eq. (18) was derived *with no input of information about the nature of the final state*.<sup>6</sup> It is therefore very tempting to immediately generalize it to other reactions. This can be done by inspection; viz., for the process  $\bar{p}p \rightarrow f + \pi^0$ , near threshold,

$$\sigma(\bar{p}p \rightarrow f + \pi^0) \cong \left(\frac{1}{2\pi}\right)^3 \left(\frac{G_A}{f_\pi}\right)^2 \left\{ \frac{R(f + \pi^0)}{R(f)} \frac{4p_{\text{c.m.}}^2}{s} \right\} \times \frac{1}{4} [\bar{\sigma}^s(\bar{p}p \rightarrow f) + \bar{\sigma}^t(\bar{p}p \rightarrow f)]. \quad (21)$$

The cross section for charged-pion emission  $\sigma(\bar{p}p \rightarrow f + \pi^+)$  is obtained from this by making the replacement

$$\frac{1}{2} [\bar{\sigma}^s(\bar{p}p \rightarrow f) + \bar{\sigma}^t(\bar{p}p \rightarrow f)] \rightarrow \frac{1}{4} [\bar{\sigma}^s(\bar{p}n \rightarrow f) + 3\bar{\sigma}^t(\bar{p}n \rightarrow f)],$$

$$\frac{R(\bar{B}B\pi^0)}{R(\bar{B}B)} \frac{4p_{\text{c.m.}}^2}{s} \cong \sqrt{2} \left(\frac{\pi}{2}\right)^2 \frac{1 - [2M_N/(2M_B + m_\pi)]^2}{(1 + m_\pi/2M_B)^{3/2}} \epsilon^2$$

$$\approx \sqrt{2} \left(\frac{1}{2}\pi\right)^2 \left\{ [1 - (M_N/M_B)^2] + \frac{1}{4} [7(M_N/M_B)^2 - 3] m_\pi/M_B - \frac{1}{32} [63(M_N/M_B)^2 - 15] (m_\pi/M_B)^2 + \dots \right\} \epsilon^2. \quad (23)$$

One usually hears the argument that only terms of lowest order in  $m_\pi/M_B$  should be retained. The point is somewhat moot; at best, the *entire calculation* is valid only to first order in  $m_\pi/M_B$ . Thus, one cannot *a priori* justify the preference of one expression to any other which is its first-order equivalent.

#### V. DATA AND DISCUSSION

Despite the approximations which have been made, there is surprisingly good agreement between the soft-pion predictions of Sec. III and some low-energy pion production data. In making these comparisons, we will assume that the core

as was done in Eq. (20).

Close to threshold, the quantity in curly brackets can be expanded to lowest order in  $\epsilon$ , the available kinetic energy. At low energies,  $n$ -body phase space is approximated by the expression<sup>15</sup>

$$R_n = \frac{(2\pi^3)^{n/2-1/2}}{2\Gamma[\frac{3}{2}n - \frac{3}{2}]} \frac{(\prod m)^{1/2}}{(\sum m)^{3/2}} \epsilon^{3n/2-5/2}, \quad (22)$$

where  $\prod m$  ( $\sum m$ ) is the product (sum) of the masses of all particles in the system. In what follows, let  $n$  be the number of particles in  $f$ .

To evaluate  $R(f)$ , set  $\epsilon = m_\pi$ . Note that the use of Eq. (22) requires the particles in  $f$  to be massive enough to remain nonrelativistic with total kinetic energy  $m_\pi$ . The numerator  $R(f + \pi)$  is evaluated by changing  $n \rightarrow n + 1$  and setting  $\epsilon = \sqrt{s} - (\sum_f M + m_\pi)$ . The ratio is then given by

$$\frac{R(f + \pi)}{R(f)} \cong (2\pi^3)^{1/2} \frac{\Gamma(\frac{3}{2}n - \frac{3}{2})}{\Gamma(\frac{3}{2}n)} m_\pi^{3-3n/2} \times \left(1 + \frac{m_\pi}{\sum_f M}\right)^{-3/2} \epsilon^{3n/2-1},$$

$$\epsilon = \sqrt{s} - (\sum_f M + m_\pi).$$

The quantity  $4p_{\text{c.m.}}^2/s$  is written more easily:

$$\frac{4p_{\text{c.m.}}^2}{s} = 1 - \frac{4M_N^2}{s} \cong 1 - \left(\frac{2M_N}{\sum_f M + m_\pi}\right)^2,$$

to lowest order in  $\epsilon$ .

In particular, for the reactions  $\bar{p}p \rightarrow \bar{B}B\pi^0$ , where  $B$  is any baryon, the low-energy expansion becomes

cross sections obey

$$\frac{1}{2}(\bar{\sigma}^s + \bar{\sigma}^t) = \frac{1}{4}(\bar{\sigma}^s + 3\bar{\sigma}^t) = \bar{\sigma},$$

for lack of evidence to the contrary. The results for  $\bar{p}p \rightarrow \bar{p}p\pi^0$ ,  $\bar{p}n\pi^+$ , and  $\bar{n}p\pi^-$  have essentially been presented in Burns *et al.*,<sup>13</sup> but for completeness they are included here in greater detail.

Exhibiting the best case first, Fig. 3 compares Eq. (20) to the combined charged-pion production cross section  $\sigma(\bar{p}p \rightarrow \bar{p}n\pi^+) + \sigma(\bar{p}p \rightarrow \bar{n}p\pi^-)$ .<sup>13,16</sup> The abscissa is scaled according to  $\ln[\epsilon(\text{GeV})]$ . The shaded region represents an estimate of the uncertainty in the soft-pion prediction due to ambiguities and uncertainties in the averaged core cross sections. We have used 30 mb  $< \bar{\sigma}(\bar{p}n \rightarrow \bar{p}n)$

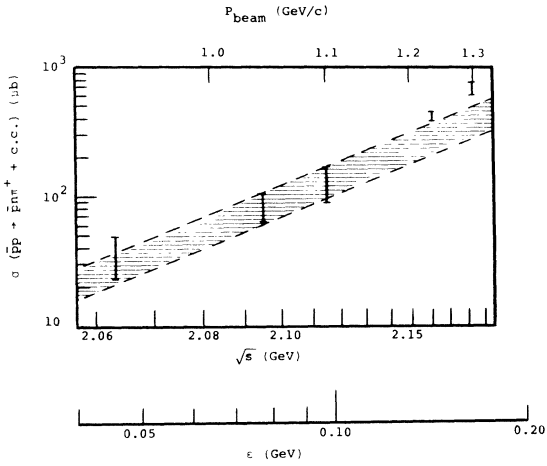


FIG. 3. Comparison between soft-pion calculations near threshold and low-energy data for  $\bar{p}p \rightarrow \bar{p}n\pi^+$ ,  $\bar{p}p \rightarrow \bar{p}n\pi^-$ . The shaded region represents an estimate of the uncertainty in the calculations (see text).

$< 50 \text{ mb}$  and  $\sigma(\bar{p}p \rightarrow \bar{p}n\pi^-) = \sigma(\bar{p}p \rightarrow \bar{p}n\pi^+)$ . The theoretical prediction is in excellent agreement with data for  $P_{\text{beam}} < 1.12 \text{ GeV}/c$ , and in reasonable agreement (within 40%) even as high as  $1.35 \text{ GeV}/c$ .

The results for  $\bar{p}p \rightarrow \bar{p}p\pi^0$ , shown in Fig. 4, are also very good below  $1.12 \text{ GeV}/c$ , but there is greater disagreement at the higher energies. In estimating the theoretical bounds, we have taken  $44 \text{ mb} < \sigma(\bar{p}p \rightarrow \bar{p}p) < 72 \text{ mb}$ .

Figures 5 and 6 compare Eq. (21) to the lowest-energy data available<sup>17</sup> on  $\bar{p}p \rightarrow \bar{\Lambda}\Lambda\pi^0$  and  $\bar{p}p \rightarrow \bar{\Sigma}^-\Sigma^+\pi^0$ . The ranges used for the core cross sections were  $22 \mu\text{b} < \sigma(\bar{p}p \rightarrow \bar{\Sigma}^-\Sigma^+) < 42 \mu\text{b}$  and  $15 \mu\text{b}$

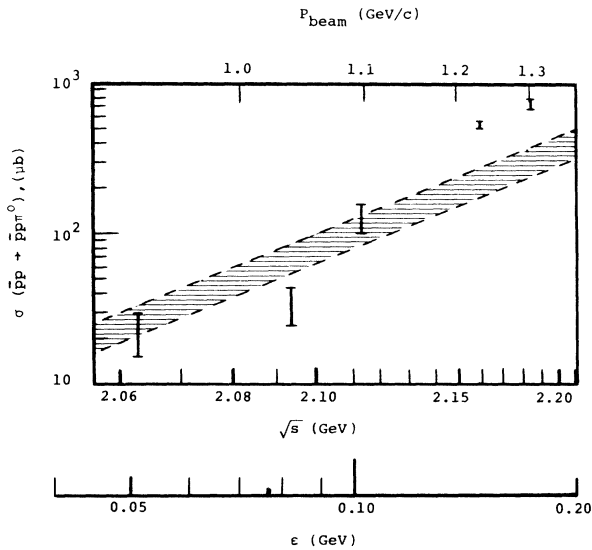


FIG. 4. Comparison between threshold calculations and data for  $\bar{p}p \rightarrow \bar{p}p\pi^0$ . See caption of Fig. 3.

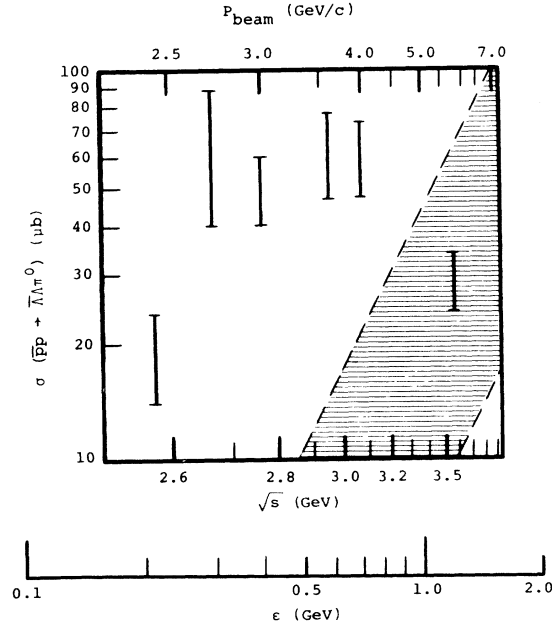


FIG. 5. Comparison between threshold calculations and data for  $\bar{p}p \rightarrow \bar{\Lambda}\Lambda\pi^0$ . See caption of Fig. 3.

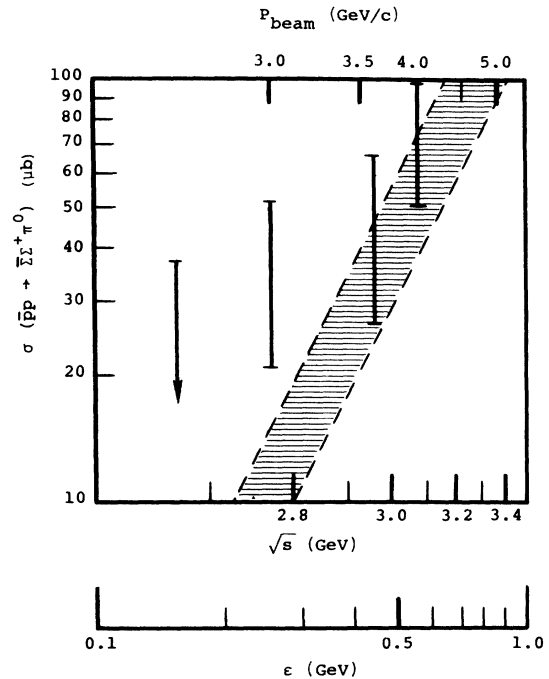


FIG. 6. Comparison between threshold calculations and data for  $\bar{p}p \rightarrow \bar{\Sigma}^-\Sigma^+\pi^0$ . See caption of Fig. 3.

$\langle \bar{\sigma}(\bar{p}p \rightarrow \bar{\Lambda}\Lambda) \rangle < 95 \mu\text{b}$ . The data for  $\bar{\Sigma}^-\Sigma^+\pi^0$  are reasonably close to the prediction, but this is not the case for  $\bar{\Lambda}\Lambda\pi^0$ , where the theoretical values are too small by one or two orders of magnitude.

The discrepancies which arise can probably be blamed on resonance formation in the final state, a problem which plagued the low-energy theorems for  $p\bar{p} \rightarrow p\bar{n}\pi^+$ .<sup>18</sup> The data of Figs. 3 and 4 are "contaminated" with  $\Delta(3,3)$  formation above the resonance threshold  $P_{\text{beam}} \gtrsim 1.26 \text{ GeV}/c$ . The sudden jump in the ratio of neutral to charged pion production above this threshold also suggests that resonance formation is a dominant mechanism; Bacon *et al.*<sup>16</sup> concluded that it accounts for the entire pion production cross section at these higher energies. Likewise, *all* the data in Figs. 5 and 6 fall above threshold for  $\Sigma^*$  and  $\Lambda^*$  resonance production. Indeed, it is remarkable that the  $\bar{\Sigma}^-\Sigma^+\pi^0$  cross sections fall as close as they do to the soft-pion prediction.

Equation (21) can be applied to more complicated reactions, but it becomes difficult to find data close enough to threshold for meaningful comparisons.<sup>19</sup> For the sake of argument, consider the processes  $\bar{p}p \rightarrow \Lambda\bar{p}K^+\pi^0$  and  $\bar{p}p \rightarrow \Sigma^+\bar{p}K^0\pi^0$ . Both have been observed<sup>20</sup> at  $P_{\text{beam}} = 5.7 \text{ GeV}/c$  with cross sections  $\sigma(\bar{p}p \rightarrow \Lambda\bar{p}K^+\pi^0 + \text{c.c.}) = 30 \pm 3 \mu\text{b}$  and  $\sigma(\bar{p}p \rightarrow \Sigma^+\bar{p}K^0\pi^0 + \text{c.c.}) = 19 \pm 4 \mu\text{b}$ . The prediction is

$$\begin{aligned} \sigma(\bar{p}p \rightarrow \Lambda\bar{p}K^+\pi^0) &\approx 4.6 \bar{\sigma}(\bar{p}p \rightarrow \Lambda\bar{p}K^+) \epsilon^{7/2}, \\ \sigma(\bar{p}p \rightarrow \Sigma^+\bar{p}K^0\pi^0) &\approx 4.9 \bar{\sigma}(\bar{p}p \rightarrow \Sigma^+\bar{p}K^0) \epsilon^{7/2}. \end{aligned} \quad (24)$$

At best, only rough estimates of the core cross sections can be made. If we take<sup>20,21</sup>

$$\begin{aligned} \bar{\sigma}(\bar{p}p \rightarrow \Lambda\bar{p}K^+ + \text{c.c.}) &\approx 25-35 \mu\text{b}, \\ \bar{\sigma}(\bar{p}p \rightarrow \Sigma^+\bar{p}K^0 + \text{c.c.}) &\approx 10-25 \mu\text{b}, \end{aligned}$$

then Eqs. (24) become

$$\begin{aligned} \sigma(\bar{p}p \rightarrow \Lambda\bar{p}K^+\pi^0 + \text{c.c.}) &\approx 71-99 \mu\text{b}, \\ \sigma(\bar{p}p \rightarrow \Sigma^+\bar{p}K^0\pi^0 + \text{c.c.}) &\approx 21-54 \mu\text{b}. \end{aligned}$$

The first is too high by a factor of 2 or 3, but the second overlaps the experimental value. However, the data were not taken close to threshold, and other (resonance) processes can be expected to significantly affect the results.

At the very least, the soft-pion model is seen to agree with  $\bar{p}p \rightarrow \bar{N}N\pi$  data close to threshold. At this low energy, the rise in cross section essentially comes from phase-space growth, and soft-pion physics determines the ratio  $\sigma/R(\bar{N}N\pi)$  in the limit  $\epsilon \rightarrow 0$ . It may do just as well for the other final states considered—certainly, the comparison to  $\bar{\Sigma}^-\Sigma^+\pi^0$  in Fig. 6 is encouraging—but available data are at energies too high to decide the issue.

#### ACKNOWLEDGMENTS

I would like to thank Professor J. Schultz for his valued help and encouragement as well as for critically reading the original manuscript. Also gratefully acknowledged are several useful discussions with Professor M. Bander and Dr. R. R. Burns.

#### APPENDIX A: SYMMETRIES

There are fourteen charge-conserving processes  $\bar{N}N \rightarrow \bar{N}N\pi$ . Using  $G$  invariance and  $C$  invariance, they can be collected into five  $G$ - $C$  equivalence classes, as shown below:

$$\begin{aligned} \mathfrak{M}(\bar{p}n\pi^+ | \bar{p}p) &= \mathfrak{M}(n\bar{p}\pi^+ | n\bar{n}) \\ &\quad \parallel \quad \parallel \\ -\mathfrak{M}(\bar{p}\bar{n}\pi^- | \bar{p}\bar{p}) &= -\mathfrak{M}(\bar{n}p\pi^- | \bar{n}n), \end{aligned} \quad (A1a)$$

$$\begin{aligned} \mathfrak{M}(\bar{p}p\pi^- | \bar{p}n) &= \mathfrak{M}(n\bar{n}\pi^- | n\bar{p}) \\ &\quad \parallel \quad \parallel \\ -\mathfrak{M}(\bar{p}\bar{p}\pi^+ | \bar{p}\bar{n}) &= -\mathfrak{M}(\bar{n}n\pi^+ | \bar{n}p), \end{aligned} \quad (A1b)$$

$$\begin{aligned} \mathfrak{M}(\bar{p}p\pi^0 | \bar{p}p) &= -\mathfrak{M}(n\bar{n}\pi^0 | n\bar{n}) \\ &\quad \parallel \quad \parallel \\ \mathfrak{M}(\bar{p}\bar{p}\pi^0 | \bar{p}\bar{p}) &= -\mathfrak{M}(\bar{n}n\pi^0 | \bar{n}n), \end{aligned} \quad (A1c)$$

$$\begin{aligned} \mathfrak{M}(\bar{n}n\pi^0 | \bar{p}p) &= -\mathfrak{M}(\bar{p}\bar{p}\pi^0 | n\bar{n}) \\ &\quad \parallel \quad \parallel \\ \mathfrak{M}(n\bar{n}\pi^0 | \bar{p}\bar{p}) &= -\mathfrak{M}(\bar{p}\bar{p}\pi^0 | \bar{n}n), \end{aligned} \quad (A1d)$$

$$\begin{aligned} \mathfrak{M}(\bar{p}n\pi^0 | \bar{p}n) &= -\mathfrak{M}(n\bar{p}\pi^0 | n\bar{p}) \\ &\quad \parallel \quad \parallel \\ \mathfrak{M}(\bar{p}\bar{n}\pi^0 | \bar{p}\bar{n}) &= -\mathfrak{M}(\bar{n}p\pi^0 | \bar{n}p). \end{aligned} \quad (A1e)$$

In each class, the horizontal equalities follow from  $G$  invariance while the vertical ones follow from  $C$  invariance. The position of a particle label in the amplitude implies its momentum and polarization. For example, in the top two amplitudes, the neutron in one final state has the momentum and polarization of the antiproton in the other.

From this alone, the number of independent amplitudes is reduced to five. However, from isotopic-spin considerations, only three of these can be linearly independent. The initial state must be in one of two isospin-invariant subspaces, a singlet or a triplet. The final state must be either in a quintuplet, in a singlet, or in one of two possible triplet subspaces. The quintuplet is of no consequence, since it cannot couple into the initial state. This leaves only three independent transition amplitudes; one between isotopic singlets, and two between isotopic triplets.

There are three ways of coupling the final-state particles together, each one leading to a different definition of the two isospin triplet amplitudes. We choose to first couple the  $\bar{N}N$  subsystem together.

That is,

$$\begin{aligned} (2^* \otimes 2) \otimes 3 &= (1 \oplus 3) \otimes 3, \\ &= (1 \otimes 3) \oplus (3 \otimes 3), \\ &= 3' \oplus (5 \oplus 3 \oplus 1). \end{aligned}$$

Let  $\mathfrak{M}'_1$  be the transition amplitude in the  $3'$  family, as defined above, and let  $\mathfrak{M}_1$  and  $\mathfrak{M}_0$  be the amplitudes in the  $3$  and  $1$  families.

It is now a simple exercise to use the Clebsch-Gordan coefficients to relate  $\mathfrak{M}_0$ ,  $\mathfrak{M}_1$ , and  $\mathfrak{M}'_1$  to representative amplitudes from the five G-C classes. These linear relationships are summarized by the matrix equation

$$\begin{pmatrix} \mathfrak{M}(\bar{p}n\pi^+ | \bar{p}p) \\ \mathfrak{M}(\bar{p}p\pi^- | \bar{p}n) \\ \mathfrak{M}(\bar{p}p\pi^0 | \bar{p}p) \\ \mathfrak{M}(\bar{n}n\pi^0 | \bar{p}p) \\ \mathfrak{M}(\bar{p}n\pi^0 | \bar{p}n) \end{pmatrix} = \begin{pmatrix} -\sqrt{1/6} & -\frac{1}{2} & 0 \\ 0 & \frac{1}{2} & -\sqrt{1/2} \\ \frac{1}{2}\sqrt{1/3} & 0 & -\frac{1}{2} \\ -\frac{1}{2}\sqrt{1/3} & 0 & -\frac{1}{2} \\ 0 & -\sqrt{1/2} & 0 \end{pmatrix} \times \begin{pmatrix} \mathfrak{M}_0 \\ \mathfrak{M}_1 \\ \mathfrak{M}'_1 \end{pmatrix}. \quad (\text{A2})$$

The three  $\pi^0$  production amplitudes themselves constitute a linearly independent set, so that the charged  $\pi^\pm$  amplitudes can be written in terms of them. From the solutions

$$\begin{aligned} \mathfrak{M}_0 &= \sqrt{3} [\mathfrak{M}(\bar{p}p\pi^0 | \bar{p}p) - \mathfrak{M}(\bar{n}n\pi^0 | \bar{p}p)], \\ \mathfrak{M}_1 &= -\sqrt{2} \mathfrak{M}(\bar{p}n\pi^0 | \bar{p}n), \\ \mathfrak{M}'_1 &= -\mathfrak{M}(\bar{p}p\pi^0 | \bar{p}p) - \mathfrak{M}(\bar{n}n\pi^0 | \bar{p}p), \end{aligned} \quad (\text{A3})$$

we easily get the relations

$$\begin{aligned} \sqrt{2} \mathfrak{M}(\bar{p}n\pi^+ | \bar{p}p) &= \mathfrak{M}(\bar{p}n\pi^0 | \bar{p}n) + \mathfrak{M}(\bar{n}n\pi^0 | \bar{p}p) \\ &\quad - \mathfrak{M}(\bar{p}p\pi^0 | \bar{p}p), \\ \sqrt{2} \mathfrak{M}(\bar{p}p\pi^- | \bar{p}n) &= \mathfrak{M}(\bar{p}p\pi^0 | \bar{p}p) + \mathfrak{M}(\bar{n}n\pi^0 | \bar{p}p) \\ &\quad - \mathfrak{M}(\bar{p}n\pi^0 | \bar{p}n). \end{aligned} \quad (\text{A4})$$

Note that the requirements of  $C$  invariance, as written in Eqs. (A1a) through (A1e), imply that  $\mathfrak{M}_1$  is antisymmetric under interchange of  $\bar{N}, N$  coordinates, while  $\mathfrak{M}_0$  and  $\mathfrak{M}'_1$  are symmetric. That is,

$$\begin{aligned} \mathfrak{M}_0(\bar{N}N\pi | \bar{N}N) &= \mathfrak{M}_0(\bar{N}\bar{N}\pi | N\bar{N}), \\ \mathfrak{M}_1(\bar{N}N\pi | \bar{N}N) &= -\mathfrak{M}_1(N\bar{N}\pi | N\bar{N}), \\ \mathfrak{M}'_1(\bar{N}N\pi | \bar{N}N) &= \mathfrak{M}'_1(N\bar{N}\pi | N\bar{N}). \end{aligned}$$

Finally, we can get a rough "statistical" estimate of the ratio  $R \equiv \sigma(\bar{p}p \rightarrow \bar{p}p\pi^0) / \sigma(\bar{p}p \rightarrow \bar{p}n\pi^+)$  directly from Eq. (A2). Assuming that  $|\mathfrak{M}_0| \cong |\mathfrak{M}_1|$

$\cong |\mathfrak{M}'_1|$ , and completely neglecting interference terms, we have

$$\begin{aligned} R &\cong \frac{\frac{1}{12} |\mathfrak{M}_0|^2 + \frac{1}{4} |\mathfrak{M}'_1|^2}{\frac{1}{6} |\mathfrak{M}_0|^2 + \frac{1}{4} |\mathfrak{M}'_1|^2} \\ &\cong \frac{4}{5}. \end{aligned}$$

#### APPENDIX B: A THRESHOLD CALCULATION FOR $pp \rightarrow pn\pi^+$

It is interesting to apply Eqs. (7) to the reaction  $pp \rightarrow pn\pi^+$  near threshold for comparison to the  $\bar{p}p \rightarrow \bar{p}p\pi^0$  calculation of Sec. III, and to the soft-pion calculation of Schillaci, Silbar, and Young.<sup>4</sup>

Using Eq. (7), we begin by writing the amplitude

$$\mathfrak{M}(pn\pi^+ | pp) = \frac{iG_A}{f_\pi} \sqrt{2} [Z_1 M(pn|np) + Z_2 M(pn|pn) - Z_4 M(pp|pp)]. \quad (\text{B1})$$

[Nucleon indexing is the same as in Sec. III; namely,  $M(N_3 N_4 | N_1 N_2)$ .] If we now introduce the isospin amplitudes

$$\begin{aligned} M(pn|np) &= \frac{1}{2}(M_1 - M_0), \\ M(pn|pn) &= \frac{1}{2}(M_1 + M_0), \\ M(pp|pp) &= M_1, \end{aligned} \quad (\text{B2})$$

then Eq. (B1) becomes

$$\begin{aligned} \mathfrak{M}(pn\pi^+ | pp) &= \frac{iG_A}{f_\pi} [\sqrt{\frac{1}{2}} (Z_1 + Z_2) M_1 \\ &\quad - \sqrt{\frac{1}{2}} (Z_1 - Z_2) M_0 - \sqrt{2} Z_4 M_1] \\ &\cong \frac{iG_A}{f_\pi} \sqrt{2} \frac{p_{c.m.}}{\sqrt{s}} \\ &\quad \times [(h_1 + h_2) M_1 - (h_1 - h_2) M_0]. \end{aligned} \quad (\text{B3})$$

The second equation follows from the first by using the threshold approximations [Eqs. (12) and (13)].

Like Eq. (11b), Eq. (B3) exhibits spin-isospin correlations, but now the  $I=1$  core contributes when  $h_1 = h_2$ , while the  $I=0$  core contributes when  $h_1 = -h_2$ . Again, because these two conditions are mutually exclusive, there is no mixing between  $M_1$  and  $M_0$  at threshold.

The next step is to arrange the four possible initial-spin states into singlet and triplet configurations, as in Sec. III. Assuming that each triplet state contributes the same squared amplitude, at least in an average sense, the sum over spins can be written as follows:

$$\begin{aligned} \sum_{\text{spins}} |\mathfrak{M}(pn\pi^+ | pp)|^2 &= \left(\frac{G_A}{f_\pi}\right)^2 \frac{4p_{c.m.}^2}{s} \\ &\quad \times \frac{1}{2} \sum_{\text{final spins}} (|M_1^s|^2 + |M_1^t|^2 + 2|M_0^t|^2). \end{aligned}$$

(Of course, the superscripts refer to spin singlet and triplet, and subscripts refer to isospin singlet and triplet.)

The final result can be written by inspection in analogy to Eqs. (15) and (19):

$$\sigma(pp \rightarrow pn\pi^+) \cong \frac{1}{32\sqrt{2}\pi} \left(\frac{G_A}{f_\pi}\right)^2 \frac{m_\pi}{M} \frac{1}{4}(\bar{\sigma}_1^s + \bar{\sigma}_1^t + 2\bar{\sigma}_0^t) \epsilon^2,$$

where the cross sections in parentheses refer to the  $NN \rightarrow NN$  core. This expression compares favorably to the one derived by Schillaci, Silbar, and Young by a somewhat more involved route. The only difference is that the term  $\bar{\sigma}_1^t$  does not appear there because of their restriction to S-wave scattering; i.e.,  $\bar{\sigma}_1^t$  contains odd partial waves only, due to Fermi statistics.

\*Work supported in part by the U.S.E.R.D.A.

<sup>1</sup>P. Nuthakki and R. A. Uritam, Phys. Rev. D 8, 3196 (1973).

<sup>2</sup>G. W. Intemann and G. K. Greenhut, Phys. Rev. D 10, 3653 (1974).

<sup>3</sup>D. S. Beder, Nuovo Cimento 56A, 625 (1968).

<sup>4</sup>M. E. Schillaci, R. R. Silbar, and J. E. Young, Phys. Rev. 179, 1539 (1969).

<sup>5</sup>R. Baier and H. Kühnelt, Nuovo Cimento 63A, 135 (1969).

<sup>6</sup>We assume throughout that only strong interactions take place in the core.

<sup>7</sup>S. L. Adler, Phys. Rev. 137, B1022 (1965); 139, B1638 (1965).

<sup>8</sup>Due to Professor J. Schultz.

<sup>9</sup>Y. Nambu and D. Lurié, Phys. Rev. 125, 1429 (1962).

<sup>10</sup>S. Fubini and G. Furlan, Ann. Phys. (N.Y.) 48, 322 (1968).

<sup>11</sup>J. E. Young, Ann. Phys. (N.Y.) 56, 391 (1970).

<sup>12</sup>M. K. Banerjee *et al.*, Phys. Rev. C 3, 509 (1971).

<sup>13</sup>R. R. Burns *et al.*, Phys. Rev. D 11, 1004 (1975).

<sup>14</sup>A comment on this point made in Burns *et al.* (Ref. 13) was not correct.

<sup>15</sup>E. Byckling and K. Kajantie, *Particle Kinematics* (Wiley, New York, 1973).

<sup>16</sup>T. C. Bacon *et al.*, Nucl. Phys. B32, 66 (1971).

<sup>17</sup>J. Badier *et al.*, Phys. Lett. B25, 152 (1967); G. P. Fisher *et al.*, Phys. Rev. 161, 1335 (1967); B. Musgrave *et al.*, Nuovo Cimento 35, 735 (1965); H. W. Atherton *et al.*, Nucl. Phys. B29, 477 (1971).

<sup>18</sup>M. E. Schillaci and R. R. Silbar, Phys. Rev. D 2, 1220 (1970).

<sup>19</sup>We have concentrated on  $\bar{p}p$  interactions in this paper. It is clear that a similar analysis can be carried out for  $pp$  interactions with various final states.

<sup>20</sup>R. K. Boeck *et al.*, Phys. Lett. 17, 166 (1965).

<sup>21</sup>C. Baltay *et al.*, Phys. Rev. 140, B1027 (1965); C. Y. Chien *et al.*, *ibid.* 152, 1171 (1966).